FEBS Letters 582 (2008) 2768–2772

Deletion of the autoregulatory insert modulates intraprotein electron transfer in rat neuronal nitric oxide synthase

Changjian Feng[a,*], Linda J. Roman[b], James T. Hazzard[c], Dipak K. Ghosh[d], Gordon Tollin[c], Bettie Sue S. Masters[b]

[a] College of Pharmacy, University of New Mexico, Albuquerque, NM 87131, United States
[b] Department of Biochemistry, The University of Texas Health Science Center at San Antonio, San Antonio, TX 78229-3900, United States
[c] Department of Biochemistry and Molecular Biophysics, University of Arizona, Tucson, AZ 85721, United States
[d] Department of Medicine, Duke University and VA Medical Centers, Durham, NC 27705, United States

Received 20 June 2008; revised 3 July 2008; accepted 4 July 2008

Available online 14 July 2008

Edited by Peter Brzezinski

Abstract Comparative CO photolysis kinetics studies on wild-type and autoregulatory (AR) insert-deletion mutant of rat nNOS holoenzyme were conducted to directly investigate the role of the unique AR insert in the catalytically significant FMN–heme intraprotein electron transfer (IET). Although the amplitude of the IET kinetic traces was decreased two- to three-fold, the AR deletion did not change the rate constant for the calmodulin-controlled IET. This suggests that the rate-limiting conversion of the electron-accepting state to a new electron-donating (output) state does not involve interactions with the AR insert, but that AR may stabilize the output state once it is formed.

Keywords: Electron transfer; Nitric oxide synthase; Kinetic

1. Introduction

In mammals, NO is synthesized by nitric oxide synthase (NOS), a homodimeric flavo-hemoprotein that catalyzes the 5-electron oxidation of L-arginine (Arg) to NO and L-citrulline with NADPH and O_2 as co-substrates [1]. There are three mammalian NOS isoforms: endothelial NOS (eNOS), neuronal NOS (nNOS), and inducible NOS (iNOS). Eukaryotic NOSs are modular heme- and flavin-containing enzymes that produce NO by very intricately-controlled redox processes [2]. It is well established that intraprotein interdomain electron transfer (IET) processes are key steps in NO synthesis through coupling reactions between the flavins and heme domains [1,3,4]. Unlike iNOS, eNOS and nNOS synthesize NO in a Ca^{2+}/CaM-dependent manner: CaM-binding triggers the IET from FMN hydroquinone ($FMNH_2$) to the catalytic heme iron in the oxygenase domain of the other subunit of the NOS dimer [5,6]. This reaction is essential for NO synthesis, and is under extraordinary control; the control mechanism of this IET is of particular interest in this study. It is generally accepted that CaM-binding has little or no effect on the thermodynamics of redox processes in NOS [7–9], indicating that the kinetic regulation of the IET processes within the enzyme by CaM binding is accomplished dynamically through controlling redox-linked conformational changes required for effective IET.

An "FMN-domain tethered shuttle" model was originally proposed by Ghosh and Salerno [10], and strongly supported by recent IET kinetic studies [11–13], that involves the swinging of the FMN domain from its original electron-accepting (input) state to a new electron-donating (output) state (Fig. 1). The IET kinetics between the catalytically significant redox couples of FMN and heme in truncated NOS constructs [12,13] and nNOS holoenzyme [11] have been directly determined by CO photolysis. These studies have shown that, even in the presence of CaM, the nNOS holoenzyme is primarily in the input state, in which the rate constant for FMN–heme IET is smaller than that in the oxyFMN construct due to the rate-limiting additional step of conversion of the input state to the output state.

Increasing evidence shows that the nNOS/eNOS-unique autoregulatory (AR) insert within the FMN domain exerts its regulatory function by stabilizing certain NOS states via interdomain interactions. Identified originally from sequence alignments and modeling and postulated to restrict alignment of the FMN binding domain with the oxygenase and/or FAD binding domains [14], this AR insert, in the absence of CaM, locks the FMN binding domain to the reductase complex via a network of hydrogen bonds so as to obstruct enzyme activation [15]. When CaM binds to the linker between the FMN and oxygenase domains at high [Ca^{2+}], the AR insert is proposed to be displaced so that the enzyme can be activated [14]. Importantly, recent studies by Roman and Masters further suggest that the AR insert is also involved in stabilizing the "open" conformation of the FMN domain for NO synthesis (i.e., the NOS output state) [16]. They proposed that, rather than being only an inhibitory element as was originally suggested [14], upon NADPH oxidation and in the presence of CaM, the AR insert interacts with CaM to stabilize the output conformation [16].

*Corresponding author.
E-mail addresses: cfeng@salud.unm.edu (C. Feng), gtollin@u.arizona.edu (G. Tollin), masters@uthscsa.edu (B.S.S. Masters).

Abbreviations: NOS, nitric oxide synthase; nNOS, neuronal NOS; CaM, calmodulin; AR, autoregulatory insert within the FMN domain of nNOS; nNOS-AR, AR-deletion mutant of nNOS; oxyFMN, two-domain NOS construct in which only the heme-containing oxygenase and FMN domains are present; nNOSoxy, nNOS oxygenase construct; IET, intraprotein electron transfer; dRF, 5-deazariboflavin; H_4B, 6R-5,6,7,8-tetrahydrobiopterin

0014-5793/$34.00
doi:10.1016/j.febslet.2008.07.005

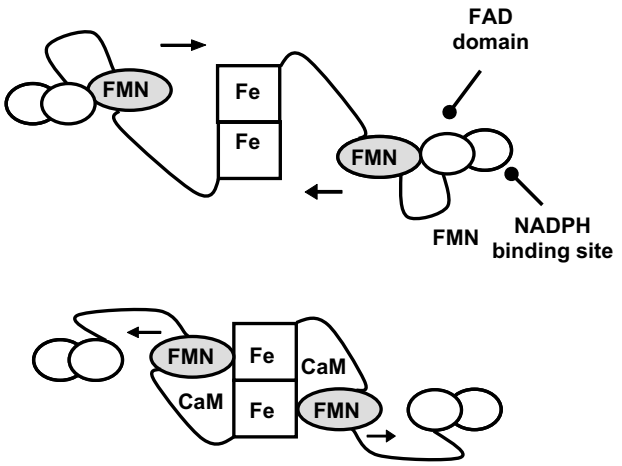

Fig. 1. Tethered shuttle model: FMN-binding domain shuttles between the NADPH-FAD-binding domain and the heme-containing oxygenase domain. The two tethers correspond to the hinge region between the FMN and FAD domains, and the CaM-binding linker between the FMN and oxygenase domains. Top: input state; bottom: putative output state. The output state is envisioned as an IET-competent complex between the oxygenase and FMN-binding domains. CaM binding unlocks the 'input state', thereby enabling the FMN domain to shuttle between the two states.

In the present work, we have directly investigated the role of the AR insert in the FMN–heme IET by comparative flash photolysis studies of the wild-type (wt) and AR-deletion mutant (nNOS-AR) of a rat nNOS holoenzyme. The results suggest that the rate-limiting conversion of the input state to the output state does not involve interactions with the AR insert, but that AR may stabilize the output state once it is formed.

2. Materials and methods

2.1. Protein expression and purification

Rat nNOS and nNOS-AR were expressed and purified as previously described [16]. NO synthesis was measured by the hemoglobin capture method as described [17], with the exception that the assays were performed in a buffer containing 50 mM Tris-HCl, pH 7.4, and 100 mM NaCl. The NO synthesis rates by wt nNOS and nNOS-AR were 70 min^{-1} and 35 min^{-1}, respectively. Rat nNOSoxy construct was expressed and purified as reported earlier [18].

2.2. Analysis of FMN and FAD content

The flavin content of these proteins was analyzed as previously described [16]. Concentrations of FMN and FAD solutions were determined from their absorbance spectra (FMN, $\varepsilon_{445} = 12\,500\ M^{-1}\ cm^{-1}$; FAD, $\varepsilon_{450} = 11\,300\ M^{-1}\ cm^{-1}$). The wt nNOS had an FAD:FMN:heme ratio of 1:1:1, and that of nNOS-AR was 1:0.9:1.

2.3. Spectrophotometric methods

CO difference spectra were performed as described [16]. The molar protein concentrations for nNOS and nNOS deletion mutants were determined based on heme content *via* reduced CO difference spectra, where $\varepsilon = 100\ mM^{-1}\ cm^{-1}$ for $\Delta A_{445-470}$, and thus reflect only cysteinyl thiolate liganded, heme-bound enzyme.

2.4. Laser flash photolysis

CO photolysis experiments were performed at room temperature as previously described [11–13]; data from ~30 laser flashes were averaged. Briefly, a solution containing 20 μM 5-deazariboflavin (dRF) and 5 mM fresh semicarbazide in pH 7.6 buffer (40 mM bis-tris propane, 400 mM NaCl, 2 mM L-Arg, 20 μM 6R-5,6,7,8-tetrahydrobiopterin (H_4B), 1 mM Ca^{2+} and 10% glycerol) was degassed in a laser photolysis cell by a mixture of Ar and CO (with a mole ratio of ~3:1). Aliquots of concentrated rat nNOS protein (150 μM) were subsequently injected through a septum, and the solution was kept in ice and further purged by passing the Ar/CO mixture over the surface for 40 min to remove minor oxygen before being subjected to illumination. The nNOS solution was then illuminated for an appropriate period of time (~90 s) to obtain a partially reduced form of [Fe(II)–CO][FMNH·], a process that was followed by characteristic maxima of Fe(II)–CO and FMNH· at 446 and 580 nm, respectively.

The reduced protein was subsequently flashed with 450 nm laser excitation to dissociate CO from Fe(II)–CO, and generate a transient Fe(II) species that is able to transfer one electron to the FMNH· intramolecularly to produce $FMNH_2$ and Fe(III). This latter IET process in the wt nNOS was followed by the loss of absorbance of FMNH· at 580 nm, and the loss of absorbance of Fe(II) at 460 nm. Because the extent of the IET process in the nNOS-AR mutant was smaller, it could only be followed by the loss of absorbance at 460 nm.

3. Results

3.1. The FMN–heme IET in wt nNOS in the presence of CaM

As expected [11], CO photolysis of the partially reduced form of [Fe(II)–CO][FMNH·] results in a rapid decay (due to

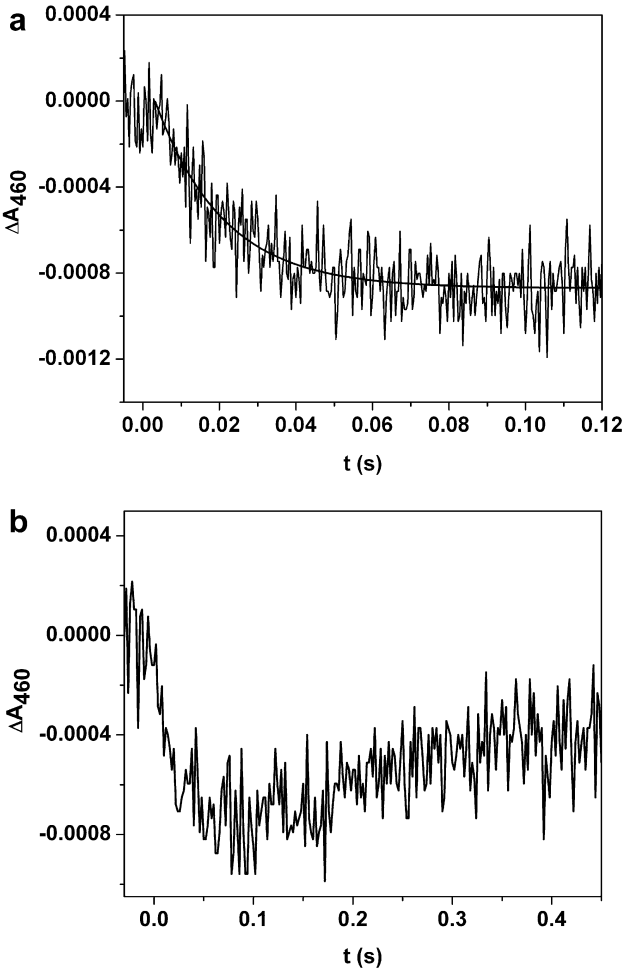

Fig. 2. Transient trace at 460 nm at (a) 0–0.12 s and (b) 0–0.5 s obtained for [Fe(II)–CO][FMNH·] form of wt nNOS with added CaM flashed by 450 nm laser excitation. Note there is a "transition" in panel b, similar to the 580 nm trace (inset of Fig. S1a in Supplementary Material). Anaerobic solutions contained 11 μM nNOS, 47 μM CaM, ~20 μM dRF, and 5 mM fresh semicarbazide in the pH 7.6 buffer. The sample was well degassed by Ar/CO (3:1) before illumination.

Table 1
The rate constants of the FMN–heme IET reaction (k_{et}^{obs}) and CO rebinding process (k_{CO}) for wt nNOS and nNOS-AR proteins[a]

	580 nm trace		460 nm trace		455 nm trace
	k_{et}^{obs} (s^{-1})	k_{CO} (s^{-1})	k_{et}^{obs} (s^{-1})	k_{CO} (s^{-1})	k_{CO} (s^{-1})
wt nNOS + CaM[b]	44 ± 5	1.8 ± 0.3	47 ± 4	2.3 ± 0.4	2.9 ± 0.3
nNOS-AR + CaM[c]	ND[d]	ND	44 ± 9	1.6 ± 0.5	7.6 ± 0.7 (77%) 1.3 ± 0.2 (23%)

[a]The IET rate constants were the average of at least ten traces with different amplitudes; data from 30 laser flashes were averaged for each trace.
[b]Excess CaM added: 11 μM wt nNOS with 47 μM CaM.
[c]Experiments were repeated at 12 μM nNOS-AR with 47 μM CaM, and 10 μM nNOS with 47 μM CaM, respectively. Signal at 580 nm was too weak to obtain a reliable fitting.
[d]ND: not determined.

the FMN–heme IET, Eq. (1)) at 580 and 460 nm below the pre-flash baseline (Fig. 2a), followed by a slow recovery to the baseline at longer time scale (due to CO re-binding to Fe(II)).

$$[Fe(II)][FMNH^{\cdot}] + [H^{+}] \rightleftharpoons [Fe(III)][FMNH_2] \quad (1)$$

Since the IET reaction is an equilibrium process, we are in fact measuring it in both directions; the CO photolysis technique follows the IET process in the reverse direction of the enzymatic turnover. We assigned the decay at 580 and 460 nm to net reduction of $FMNH^{\cdot}$ and net oxidation of heme, respectively. This assignment is supported by the fact that the absorption change due to FMNsq/hq transition is maximal at 580 nm, with an intermediate amplitude at 460 nm [19]. The details are provided in the Supplementary Material.

The observed IET rate constant (Table 1) is in good agreement with the value (38 ± 4 s^{-1}) for another preparation of wt nNOS obtained in a different laboratory [11]. The spectral "transition" (i.e., a reversal in direction of absorption changes over time) in the 460 nm trace (Fig. 2b) was absent without added CaM (data not shown), indicating no IET in the absence of CaM.

3.2. The FMN–heme IET in the nNOS-AR mutant in the presence and absence of CaM

Upon CO photolysis, the absorption of the partially reduced CaM-bound nNOS-AR at 460 nm rapidly decays below the baseline due to oxidation of Fe(II) with a rate constant of 44 ± 9 s^{-1} (Fig. 3), followed by a slow recovery toward baseline with a rate constant of 1.6 ± 0.5 s^{-1}. Importantly, the rate constant of the rapid decay at 460 nm for nNOS-AR is independent of the signal amplitude (data not shown), indicating an intra-protein process. On the other hand, a transition in the 580 nm traces for the nNOS-AR mutant could be barely observed (Inset of Fig. 3); the signals at 580 nm were very weak, and accurate values for the IET rate constant or the amplitude of the signal were not obtainable from the traces. Thus, the amplitudes of the rapid decay at 460 nm were compared for the wt and nNOS-AR proteins, in order to quantitate the differences in the amplitude of IET occurring in the two proteins.

Upon averaging four traces at 460 nm for each protein, it was found that the amplitudes of the IET traces were 0.00088 ± 0.00004 and 0.00029 ± 0.00008 for the wt and nNOS-AR proteins, respectively (see Figs. 2a and 3); although these changes are small, they are outside of the error limits. Thus there is a two- to three-fold decrease in the IET amplitude for the nNOS-AR mutant compared to the wt protein. The amplitude of the IET phase was evaluated upon the solid line fitting to the trace; the details are provided in the Supplementary Material.

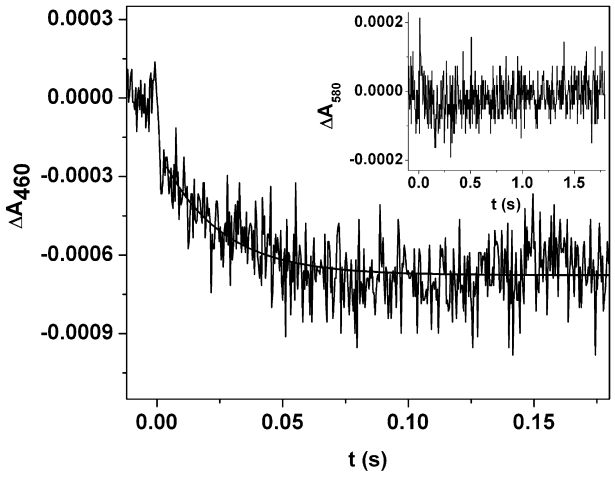

Fig. 3. Transient trace at 460 nm at 0–0.2 s obtained for [Fe(II)–CO][$FMNH^{\cdot}$] form of the nNOS-AR with added CaM flashed by 450 nm laser excitation. Inset is the 580 nm trace at 0–2 s; note that the trace was very weak, and does not have a marked transition, in contrast to the wt protein (Fig. S1 in Supplementary Material).

Fig. 4 shows the transient trace at 460 nm obtained by flashing the partially reduced nNOS-AR in the absence of CaM with the 450 nm laser excitations. Note the absence of the rapid decay, indicating no FMN–heme IET.

4. Discussion

The observed FMN–heme IET rate constant for the nNOS-AR mutant, as obtained from the 460 nm traces, is similar to that of the wt protein (Table 1). This result suggests that the rate-limiting step for this IET process does not involve interactions with the AR insert. The fact that the IET rate constant in the holoenzyme is approximately an order of magnitude smaller than that in the oxyFMN construct indicates that, in the holoenzyme, the rate-limiting step in the IET is the conversion of the shielded electron-accepting (input) state to a new electron-donating (output) state, and that the role of CaM is to allow this conversion to occur (Fig. 1) [11]. CaM unlocks the input state, thereby enabling the FMN domain to shuttle between the two enzyme states, and thus make contacts with the heme domain (Fig. 1).

Importantly, the fact that the AR-deletion does not change the rate constant for CaM-controlled FMN–heme IET (Table 1) suggests that in the nNOS holoenzyme CaM activation effectively removes the constraints imposed by the nNOS

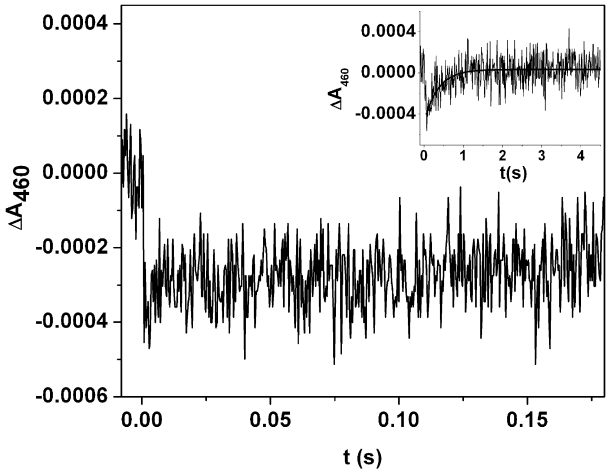

Fig. 4. Transient trace at 460 nm at 0–0.2 s for [Fe(II)–CO][FMNH] form of the nNOS-AR without added CaM flashed by 450 nm laser excitation. Note that the trace does not possess the rapid decay, in contrast to that of CaM-bound nNOS-AR at the same time scale (Fig. 3). Inset is the 460 nm trace at 0–5 s, which is due to the CO re-binding process (with a rate constant of $1.6 \pm 0.5\ s^{-1}$).

unique AR insert on the release of the FMN binding domain, at least under single turnover conditions. Furthermore, in the iNOS holoenzyme the rate constant for the IET between heme and FMN is indistinguishable from CaM-activated nNOS holoenzyme (Feng et al., unpublished data). Finally, in the nNOS holoenzyme, IET in the absence of CaM is too slow to measure [11]. Taken together, these results suggest that CaM activation effectively removes the inhibitory effects of the unique AR insert in nNOS.

Quantifications of the amplitudes of the 460 nm traces show that there is an appreciable decrease in the extent of IET in the nNOS-AR mutant. Note that the mutant has essentially a full complement of FMN (i.e., FAD:FMN:heme is 1:0.9:1), and the yield of $FMNH^{\cdot}$ is comparable to the wild-type; therefore the decrease in the IET amplitude is not due to a loss of FMN in the mutant. A plausible mechanism for this decrease is destabilization of the FMN/heme complex in the absence of the AR insert. Stated another way, the AR insert may promote interactions between the FMN and heme domains; this has the effect of increasing the population of the output state, without influencing the IET rate constant. The amplitude of the IET signal is dependent on the fraction of the FMN-binding domain that can access the output state conformation because, in the presence of CaM, the FMN-binding domain is free to shuttle between the NADPH-FAD-binding domain and the oxygenase domain (Fig. 1). Note that the FMN–heme IET is an intramolecular process, and thus its rate constant is independent of the fraction of protein in the output state. However, the amplitude of the IET will reflect the extent to which the output state can be achieved. We recognize that the amplitude level of the IET traces can only provide indirect evidence for the relative amounts of the output state in the wt and in the nNOS-AR mutant. Additional spectroscopic analysis will be required to confirm this.

It is also important to note that the IET in the nNOS-AR mutant was activated upon adding CaM (Figs. 3 and 4); this is identical to what was observed in the wt NOS [11]. It has also been shown that CaM is required for maximal NO synthesis activity in the mutant, and deletion of AR has a minimal (~25%) effect on the catalytic activity [16]. These results suggest that the CaM dependence of formation of the NOS output state also involves other intrinsic control elements.

Taken together, we propose that CaM binding is a dominant factor in controlling output state formation, while the AR insert may be also important in enhancing or stabilizing the productive docking of the FMN domain to the heme domain. The rate-limiting conversion of the input state to output state (prior to formation of the IET-competent FMN/heme complex, Fig. 1) does not involve interactions with the AR insert, as evidenced by the same IET rate constant in the AR mutants. This insert may, however, stabilize the FMN/heme complex after it is formed, as suggested by the appreciable decrease in the amplitude of the IET traces. These results need to be extended by future dynamic and structural studies in which the conformational space explored by the AR insert will be elucidated, and to provide insights into how this is changed by CaM binding without sterically blocking the interactions between the FMN and heme domains.

Acknowledgements: This work is funded by the NIH (GM07581811 and HL091280 to C.F., GM52419 and HL30050 to B.S.S.M.), and the PhRMA Foundation and UNM HSC RAC grant (to C.F.). B.S.S.M. is the Robert A. Welch Foundation Distinguished Professor in Chemistry (AQ0012). We thank Prof. John C. Salerno for helpful discussion.

Appendix A. Supplementary material

Supplementary data associated with this article can be found, in the online version, at doi:10.1016/j.febslet.2008.07.005.

References

[1] Alderton, W.K., Cooper, C.E. and Knowles, R.G. (2001) Nitric oxide synthases: structure, function and inhibition. Biochem. J. 357, 593–615.
[2] Roman, L.J., Martasek, P. and Masters, B.S.S. (2002) Intrinsic and extrinsic modulation of nitric oxide synthase activity. Chem. Rev. 102, 1179–1189.
[3] Li, H.Y. and Poulos, T.L. (2005) Structure-function studies on nitric oxide synthases. J. Inorg. Biochem. 99, 293–305.
[4] Jachymova, M. et al. (2005) Recruitment of governing elements for electron transfer in the nitric oxide synthase family. Proc. Natl. Acad. Sci. USA 102, 15833–15838.
[5] Panda, K., Ghosh, S. and Stuehr, D.J. (2001) Calmodulin activates intersubunit electron transfer in the neuronal nitric-oxide synthase dimer. J. Biol. Chem. 276, 23349–23356.
[6] Abu-Soud, H.M., Yoho, L.L. and Stuehr, D.J. (1994) Calmodulin controls neuronal nitric-oxide synthase by a dual mechanism – activation of intradomain and interdomain electron transfer. J. Biol. Chem. 269, 32047–32050.
[7] Noble, M.A. et al. (1999) Potentiometric analysis of the flavin cofactors of neuronal nitric oxide synthase. Biochemistry 38, 16413–16418.
[8] Gao, Y.T. et al. (2004) Thermodynamics of oxidation-reduction reactions in mammalian nitric-oxide synthase Isoforms. J. Biol. Chem. 279, 18759–18766.
[9] Daff, S. et al. (2001) Control of electron transfer in neuronal NO synthase. Biochem. Soc. Trans. 29, 147–152.
[10] Ghosh, D.K. and Salerno, J.C. (2003) Nitric oxide synthases: domain structure and alignment in enzyme function and control. Front. Biosci. 8, D193–D209.
[11] Feng, C.J., Tollin, G., Hazzard, J.T., Nahm, N.J., Guillemette, J.G., Salerno, J.C. and Ghosh, D.K. (2007) Direct measurement

by laser flash photolysis of intraprotein electron transfer in a rat neuronal nitric oxide synthase. J. Am. Chem. Soc. 129, 5621–5629.
[12] Feng, C.J., Tollin, G., Holliday, M.A., Thomas, C., Salerno, J.C., Enemark, J.H. and Ghosh, D.K. (2006) Intraprotein electron transfer in a two-domain construct of neuronal nitric oxide synthase: the output state in nitric oxide formation. Biochemistry 45, 6354–6362.
[13] Feng, C.J., Thomas, C., Holliday, M.A., Tollin, G., Salerno, J.C., Ghosh, D.K. and Enemark, J.H. (2006) Direct measurement by laser flash photolysis of intramolecular electron transfer in a two-domain construct of murine inducible nitric oxide synthase. J. Am. Chem. Soc. 128, 3808–3811.
[14] Salerno, J.C. et al. (1997) An autoinhibitory control element defines calcium-regulated isoforms of nitric oxide synthase. J. Biol. Chem. 272, 29769–29777.
[15] Garcin, E.D. et al. (2004) Structural basis for isozyme-specific regulation of electron transfer in nitric-oxide synthase. J. Biol. Chem. 279, 37918–37927.
[16] Roman, L.J. and Masters, B.S.S. (2006) Electron transfer by neuronal nitric-oxide synthase is regulated by concerted interaction of calmodulin and two intrinsic regulatory elements. J. Biol. Chem. 281, 23111–23118.
[17] Martasek, P., Miller, R.T., Roman, L.J., Shea, T., Masters, B.S.S. and Lester, P. (1999) Assay of isoforms of Escherichia coli-expressed nitric oxide synthase, in: Methods in Enzymology, Academic Press, pp. 70–78.
[18] Ghosh, D.K., Holliday, M.A., Thomas, C., Weinberg, J.B., Smith, S.M.E. and Salerno, J.C. (2006) Nitric-oxide synthase output state – design and properties of nitric-oxide synthase oxygenase/FMN domain constructs. J. Biol. Chem. 281, 14173–14183.
[19] Munro, A.W., Noble, M.A., Robledo, L., Daff, S.N. and Chapman, S.K. (2001) Determination of the redox properties of human NADPH-cytochrome P450 reductase. Biochemistry 40, 1956–1963.